Research Square

Preprints are preliminary reports that have not undergone peer review. They should not be considered conclusive, used to inform clinical practice, or referenced by the media as validated information.

Simulation and Estimation of Future Precipitation Changes in Arid Regions: A Case Study of Xinjiang, Northwest China

Haoyang Du
Nanjing University https://orcid.org/0000-0002-2056-4474
Manchun Li (liman12531@163.com)
Nanjing University
Penghui Jiang
Nanjing university
Haoqing Tang
Nanjing university
Xiaolong Jin
NanJing university
Dengshuai Chen
Nanjing University
Chen Zhou
Nanjing university
Dong Chen
Nanjing Tech University

Research Article

Keywords: WRF, Projected Precipitation, CCSM4, RCP4.5, RCP8.5

Posted Date: April 22nd, 2021

DOI: https://doi.org/10.21203/rs.3.rs-441462/v1

License: This work is licensed under a Creative Commons Attribution 4.0 International License.
Read Full License

Version of Record: A version of this preprint was published at Climatic Change on August 18th, 2021. See the published version at https://doi.org/10.1007/s10584-021-03192-z.

Simulation and estimation of future precipitation changes in arid regions: a case study of Xinjiang, Northwest China

Haoyang Du[1,2*], Manchun Li[1,2], Penghui Jiang[1,2], Haoqing Tang[1,2], Xiaolong Jin[1,2], Dengshuai Chen[1,2], Chen Zhou[1,2], Dong Chen[1,2]

1 School of Geography and Ocean Science, Nanjing University, Nanjing, 210023, China

2 Jiangsu Provincial Key Laboratory of Geographic Information Science and Technology, Nanjing University, Nanjing, 210023, China.

* Correspondence: liman12531@163.com; Tel.: +86-181-6801-1071

Abstract: Precipitation is critical for maintaining ecosystem stability, especially in arid regions. This study was primarily focused on the changes during the present (i.e., from 1985 to 2005) and future (i.e., from 2040 to 2059) periods in Xinjiang, northwest China. To predict the future climate, the Weather Research and Forecasting model was run in Xinjiang using National Climate Research Center Community Climate System Model version 4 for the mid-21st century under representative concentration pathways 4.5 and 8.5 (RCP4.5 and RCP8.5, respectively). The results indicate that the amount of annual precipitation would increase in the future under RCP4.5 and RCP8.5 in Xinjiang, especially in the mountainous areas. The increase in precipitation was predicted to be much smaller under RCP8.5 than under RCP4.5, except in Southern Xinjiang. Moreover, the increased precipitation predicted in Xinjiang implies that the current humid and warm conditions will continue. In addition, the largest increase in seasonal precipitation was predicted to occur in spring and summer in Tian Shan and Northern Xinjiang, whereas this phenomenon will occur in spring and winter in Southern Xinjiang. In addition, it was predicted that daily heavy precipitation events will occur more frequently in various subregions of Xinjiang, although light rain events will remain dominant. Finally, the increase in the frequency of heavy precipitation events was found to be related to the vertically integrated column precipitation, whereas the relative humidity was observed to be closely related to the changes in annual and seasonal precipitation.

Keywords: WRF; Projected Precipitation; CCSM4; RCP4.5; RCP8.5

1. Introduction

Global climate change and climate variations are significantly affected by human activities (Li et al., 2011). In the past 130 years, the earth has experienced significant warming, with the surface air temperature increasing by 0.85 °C (Solomon et al., 2007; Stocker, 2014). The rising temperature has greatly increased the amount of extreme temperature events as well as changed the pattern of global precipitation (Kharin et al., 2013). Climate change poses different risks to the ecological environments in different areas, and the degree of influence depends on the topography of the region and distance from the ocean (Wang et al., 2013).

Xinjiang is located in Northwest China with an area of 1.6×10^6 km^2, is far away from the ocean, and is surrounded by mountains (Zhang et al., 2012). Xinjiang has a typically continental and arid or semi-arid climate with an annual precipitation range from less than 50 mm in Tarim Basin to approximately 800 mm in the Tianshan Mountains (Chen et al., 2009; Domrös and Peng, 2012; Tan and Shao, 2017; Wang et al., 2013). Owing to global warming, although the total amount of annual precipitation in some areas such as the Taklamakan desert is zero in some years, Xinjiang has experienced an overall change from a warm and dry to warm and wet climate (Shi et al., 2007; Xu et al., 2010). Specifically, the average surface air temperature in Xinjiang has increased by 0.18 °C per decade in the last century, which is much higher than the global average rate (Chen et al., 2009). Meanwhile, the amount of precipitation has increased by 20–30 mm per decade (Tan and Shao, 2017). The diverse climate in Xinjiang primarily results in an obvious difference between t the desert and alpine mountain ecosystems (Li et al., 2013; Wu et al., 2010). Based on these considerations, Xinjiang has been a popular research area for exploring the interactions between local ecosystems and local climate changes.

To explain these interactions, Cao et al., (2011) demonstrated that the decrease in annual precipitation, instead of the temperature, was the main factor resulting in the vegetation coverage fluctuation in Xinjiang. Fang et al., (2013) showed that the trends in vegetation productivity during the growing season were closely to the precipitation. Seddon et al., (2016) proved that the steppe and prairie systems in Xinjiang have strong responses to precipitation anomalies. Huang et al., (2014) estimated the future changes in annual precipitation in Central Asia under different representative concentration pathways (2.6, 4.5, and 8.5) and showed that the amount of precipitation will significantly increase from 2011 to 2100. All of these previous studies have proven that climate change is closely related to the corresponding ecosystem changes.

Although current researchers have achieved sufficient improvements in their explorations of future climate change in Central Asia and spatial patterns of precipitation, a critical issue remained to be solved. Specifically, global climate models (GCMs) with coarse resolutions (i.e., >100 km) have always been used in research thus far. Consequently, detailed characteristics such as precipitation on the regional scale cannot be fully reflected. To overcome this drawback, regional climate models with high resolutions have been utilized for dynamical downscaling, using the GCMs outputs as a forcing condition to achieve detailed dynamical descriptions of regional precipitation. This approach has been proven to be efficient for Spain, the Canary Islands, China, and Central Asia (Argueso et al., 2012; Exposito et al., 2015; Liu et al., 2013; Qiu et al., 2017). However, this method has not been applied to Xinjiang for regional climate downscaling. Thus, detailed characteristics in Xinjiang, including precipitation and temperature, are unknown. Consequently, the future climate change trends cannot be efficiently revealed and the changes in hydrology and ecosystems caused by climate change cannot be reasonably addressed.

To overcome this issue, this study aimed to investigate the changes in the intensity and frequency of precipitation under different emission scenarios in Xinjiang in the future decades of the 21st century. Specifically, we obtained the climate change data by using the Weather Research and Forecast (WRF) model version3.8.1 at 10 km resolution in the mid-21st century in Xinjiang (Skamarock and W. Wang, 2008). The initial and boundary conditions of the WRF model were derived from simulations performed using National Climate Research Center (NCAR) Community Climate System Model version 4 (CCSM4) under representative concentration pathways 4.5 and 8.5 (RCP4.5 and RCP8.5, respectively). RCP 4.5 and RCP8.5 represent long-term global greenhouse gas emissions that stabilize radiation at 4.5 W/m^2 (approximately 650 ppm CO_2 equivalent) and 8.5 W/m^2 (approximately 1370 ppm CO2 equivalent) (Gent et al., 2011).

The strucutre of this paper is organized as follows. Section 2 describes the details of the WRF configuration and GCM output. Section 3 presents the validation of the WRF model in Xinjiang and the predicted precipitation results between the mid-21st century and the past 20 years, discuss the differences from the current climate, and details the atmospheric processes these changes. Section 4 dicuss the uncertainty of modern-era retrospective analysis for research and applications (MERRA) data, the difference between WRF and CCSM4, and the effect of topography on precipitation. Finaly, section 5 summarizes the main findings of this work.

2. Experimental Design, Data, and Methodology

2.1 WRF model and experimental design

The WRF model is a high-resolution mesoscale prediction model and data assimilation system that is widely used in climate change research (Bao et al., 2015; Exposito et al., 2015). In this study, WRF version 3.8.1 was employed to downscale dynamically GCM outputs with coarse resolution and to generate high-resolution data for physical processes on the regional scale, especially in complex surface areas with heterogeneous land cover and topography (Chen and Frauenfeld, 2016). The initial and lateral boundary conditions used to drive the WRF model were derived from CCSM4 RCP4.5 and RCP8.5, which have horizontal resolutions of 0.9°×1.25° (longitude and latitude) for the years 2039–2059. The average precipitation in the future was compared with the average precipitation from 1985 to 2005, which was also dynamically downscaled by WRF using historical CCSM4 data. The staring years of the present and future simulations, (i.e., 1985 and 2039), were regarded as the model spin-up and discarded. As shown in Fig. 1, two one-way nested model domains with 124×135 and 241×199 horizontal grid points and spatial separations of 30 km and 10 km were configured with 28 vertical levels reaching 50 hPa. The map projection was Lambert conformal, and the central point was located at 41.4°N, 84.8°E. The inner domain provides full coverage of the Xinjiang region. Based on prior research (Qiu et al., 2017), the following parameterization schemes were used in WRF configuration : the Betts-Miller-Janjić scheme for cumulus parameterization (Janjić, 1994); cloud microphysics scheme of Thompson(Thompson et al., 2008); land surface parameterization scheme using the Noah land surface model (LSM), which provides the four-layer soil temperature and moisture model (Chen and Dudhia, 2001), and the Mellor-Yamada-Janjić scheme for the planetary boundary layer(Janjić, 2002). In addition, the NCAR community atmosphere model (CAM) was used to calculate the atmospheric longwave and shortwave radiation transfer (Collins et al., 2004).

2.2 Data

To assess the capabilities of current climate model simulations, observational data were used to validate the WRF model outputs qualitatively and quantitatively in this study. Ground-based meteorological observation data describing the daily as well as average, maximum, and minimum precipitation from 69 meteorological stations were obtained from the China Meteorological Data Sharing Service System (http://cdc.cma.gov.cn). The observed data covered the period from 1985 to 2005, and we empolyed the following process to inspect these data with high quality (Li et al., 2012). First, we eliminated the observed stations with more than 25% missing data were eliminated throughout the verification process. Second, we removed the stations that had missing data for two more months per year were removed. Through this process, the observed data from 54 meteorological stations were retained and empolyed in our experiments and analysis (Table 1). As there are few stations in the mountains, specifically in South Xinjiang, the MERRA data (Rienecker et al., 2011), which compare the most favorably among multiple datasets with ground observations, were compared with the model results (Hu et al., 2016), as a supplement to the observational data.

2.3 Regionalization method

There numerous of types of climates in Xinjiang due to its complex topography. Therefore, it is necessary to divide this area into subregions to explore the effectiveness of the WRF. To identify and classify efficiently the subregions that have similar climate patterns, the well-known cluster analysis method (Duque et al., 2007) has been proven to be sufficiently effective to achieve this objective in Central Asia (Qiu et al., 2017) and the Tianshan Mountains (Chen et al., 2019). The K-nearest neighbor (KNN) method was employed to divide the region further into subregions based on the monthly mean precipitation data from 54 ground stations. To obtain the optimal spatial constraint parameters, we used a series of K values ranging from 2 to 10. The cluster analysis tool can automatically reveal the number of clusters by finding the climate characteristics with the highest similarity (Zhang et al., 2018). The Calinski Harabasz pseudo F-statistic can be automatically measured to quantify the similarity and dissimilarity between groups (Caliński and Harabasz, 1974; Qiu et al., 2017; Zhang et al., 2018). F can be calcualted using:

$$\mathrm{F} = \frac{\frac{R^2}{n_C-1}}{\frac{1-R^2}{n-n_c}}, \tag{1}$$

where $R^2 = \frac{BGD-WGS}{BGD}$ and a larger value indicates a better clustering result. WGS reflects the within-cluster similarity cluster, and BGD reflects the between-cluster difference. The formulas for WGS and BGD are as follows:

$$\mathrm{BGD} = \sum_{i=1}^{n_c} \sum_{j=1}^{n_i} \sum_{k=1}^{n_v} (v_{ij}^k - v_j^k)^2, \tag{2}$$

and

$$\mathrm{WGS} = \sum_{i=1}^{n_c} \sum_{j=1}^{n_i} \sum_{k=1}^{n_v} \left(v_{ij}^{k} - v_{i}^{k}\right)^2, \quad (3)$$

where

n = number of objects to be regionalized.

n_i = number of objects in cluster i.

n_c= number of clusters.

n_v= number of variables used to cluster objects.

v_{ij}^k= value of the kth variable of the jth object in the ith cluster.

v_i^k= mean value of the kth variable.

v_j^k=mean value of the kth variable in cluster j.

During the cluster analysis, when K=8 and the number of category was set to 3, R^2 and F reached the optimal values of 0.81 and 83.26, respectively. Hence, in our experiments, K = 8 was used as the spatial constraint of the KNN algorithm, and three climate subregions in Xinjiang were obtained: Northern Xinjiang, the Tianshan Mountains, and Southern Xinjiang (Fig. 1). The subregions identified in this area are similar to those described in (Zhang et al., 2017).

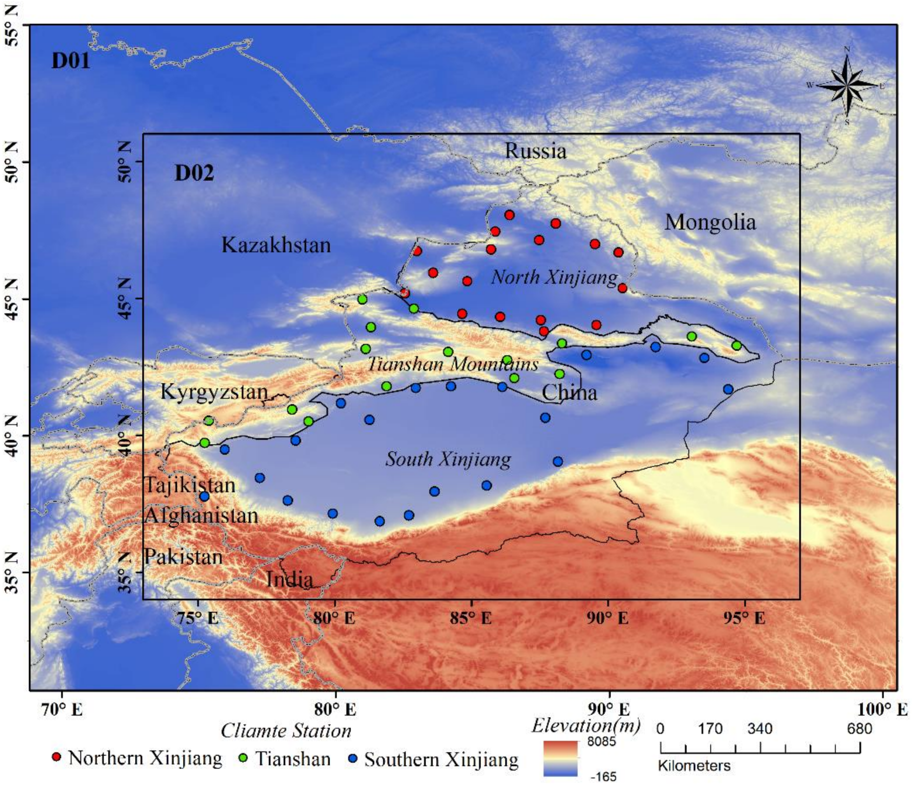

Fig. 1. Simulated domain (**D01**) 50 km and (**D02**) 10 km of WRF and the ground meteorological stations with consistent precipitation variations in the study area (**D02**).

3. Results

3.1 Evaluation of the simulation results

3.1.1 Annual and seasonal precipitation

Fig. 2 shows the spatial distributions of the annual and seasonal average precipitation in

Xinjiang from CCSM4, MERRA, and WRF for 1986–2005. Compared to the CCSM4 data, WRF downscaling of the annual and seasonal precipitation in Xinjiang can provide a more detailed spatial pattern of precipitation. The most striking spatial patterns are observed along the Tianshan Mountains, Altay Mountains, and across the Tarim Basin (desert). In the WRF simulations results, detailed terrain-induced features in precipitation patterns can be observed (Chen et al., 2019). The WRF model clearly reflects the heterogeneous spatial patterns in the precipitation data, especially in the Tianshan Mountains and Tarim Basin (Figs. 2 c, f, i, l, and o). These features are also observed in the MERRA reanalysis results (Figs. 2 b, e, h, k, and n). Although the CCSM4 data slightly underestimated the precipitation in Tianshan, they significantly overestimated the precipitation in Southern and Northern Xinjiang. Therefore, they overestimated the total precipitation in all of Xinjiang. The overestimation of precipitation also occurred in many other GCMs (Bao et al., 2015; Flato et al., 2014). Moreover, compared to the CCSM4 data, the precipitation data simulated by the WRF model are more consistent with MERRA precipitation results, with a high spatial correlation coefficient of 0.82–0.92 (CCSM4, 0.68–0.80) and low relative bias of 12%–30% (CCSM4, 33%–57%) in annual and seasonal data (Table 1).

Table 1: Spatial correlation coefficient and relative bias for annual and seasonal precipitation in Xinjiang between CCSM4 or WRF simulation and MERRA data. ANN stands for annual, MAM for March-April-May, JJA for June-July-August, SON for September-October-November, and DJF for December-January-February.

	Pattern Correlation		**Relative Bias (%)**	
	CCSM4	**WRF**	**CCSM4**	**WRF**
ANN	0.73	0.89	39	12
MAM	0.70	0.87	46	15
JJA	0.80	0.92	33	22
SON	0.73	0.90	50	26
DJF	0.68	0.82	57	30

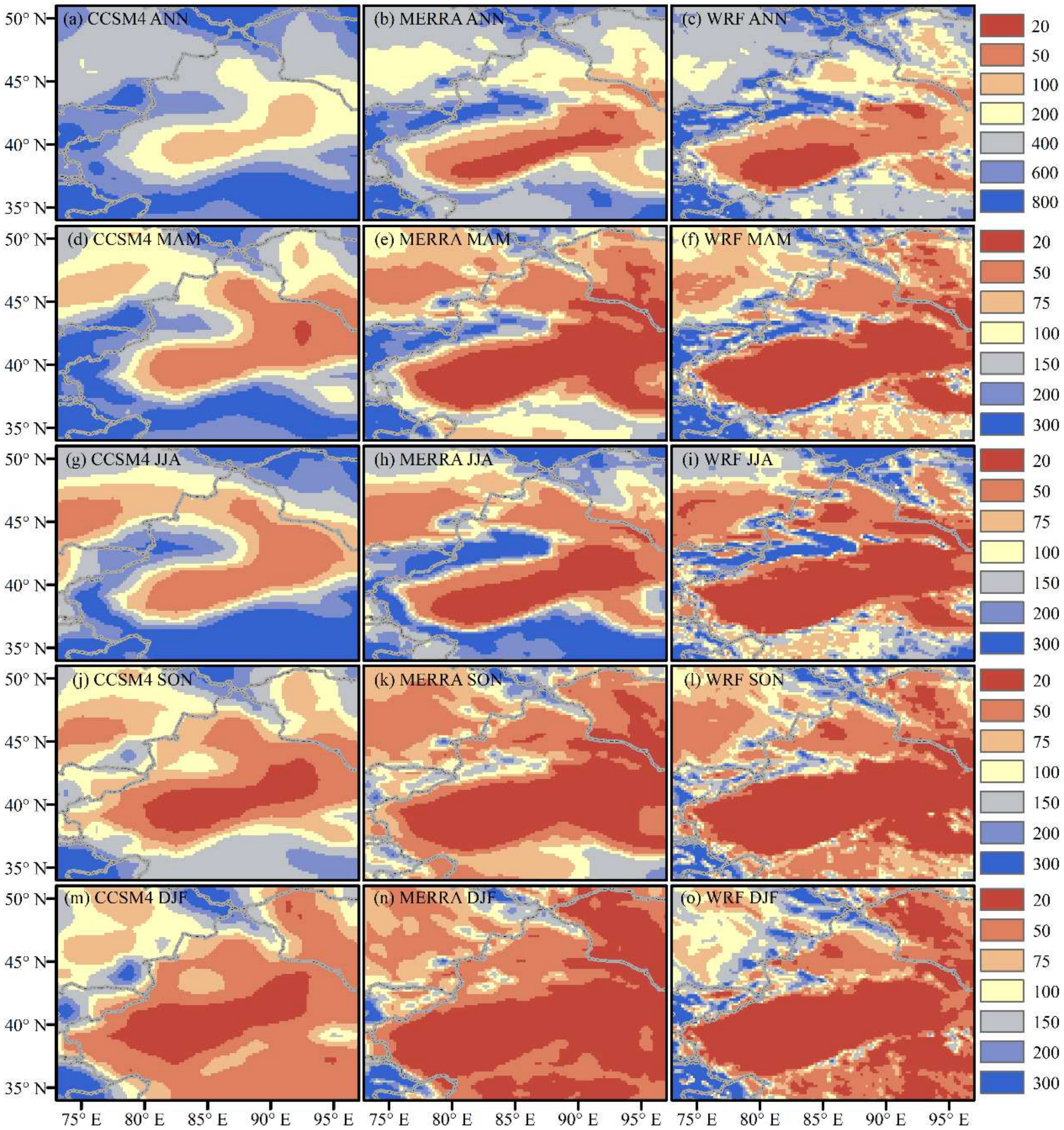

Fig. 2. Mean annual and seasonal spatial patterns of precipitation for 1986–2005 derived from CCSM4 simulation (**a,d,g,j,m**), MERRA reanalysis data (**b,e,h,k,n**), and WRF simulation (**c,f,i,l,o**). ANN: annual (**a–c**), MAM: spring (**d–f**), JJA: summer (**g–i**), SON:autumn (**j–l**), DJF: winter (**m–o**).

3.1.2 Monthly precipitation and daily precipitation events

Figs. 3 a–c display the annual cycles of precipitation averaged over the three subregions. As mentioned in Section 3.1.1, compared to the CCSM4 data, which overestimated the precipitation amounts in Southern and Northern Xinjiang and underestimates precipitation in Tianshan, the WRF data perfectly captured the annual precipitation change cycles in the three subregions (Figs. 3a–c). The CCSM4 data significantly overestimated the precipitation during the annual cycles in Southern and Northern Xinjiang, which is the main reason that the CCSM4 data overestimated precipitation in Xinjiang, whereas the WRF approach corrected this deviation and the corresponding data agreed with the observations (Figs. 3a and b).

To assess the accuracy of the WRF simulated daily precipitation, we defined a metric. We started with the precipitation accumulated during daily events in a particular intensity range. These ranges are from 1–5 mm day^{-1} to 35–40 mm day^{-1}, increasing by 5 mm day^{-1} (Figs. 3d–f). The contribution to the annual precipitation from each intensity group was used as the metric to describe the daily precipitation intensity profile. This metric is analogous to the precipitation probability density function used in Argueso et al., (2012). Figs. 3d–f shows the amount of annual precipitation grouped by events over Southern Xinjiang, Northern Xinjiang, and Tianshan. Each value indicates how much precipitation is caused by the events of a particular intensity. Compared to the CCSM4 distribution, the WRF simulated distribution more closely describes the observed data. Although the WRF simulated daily precipitation events are still overestimated or underestimated in all three subregions, the differences are generally small. Morever, Figs. 3(d–f) shows that the precipitation in each subregion has a gamma distribution with precipitation from light events contributing the most to the annual precipitation .

To summarize, the precipitation in Xinjiang during 1986–2005 was reasonably well simulated by our configured WRF model, on daily, monthly, seasonal, and annual scales. Although some large differences existed in the transition area from the Tarim Basin to the Tibetan Plateau and in the complex terrain of the Tianshan Mountains, the WRF model still provided better correction compared to the CCSM4 data.

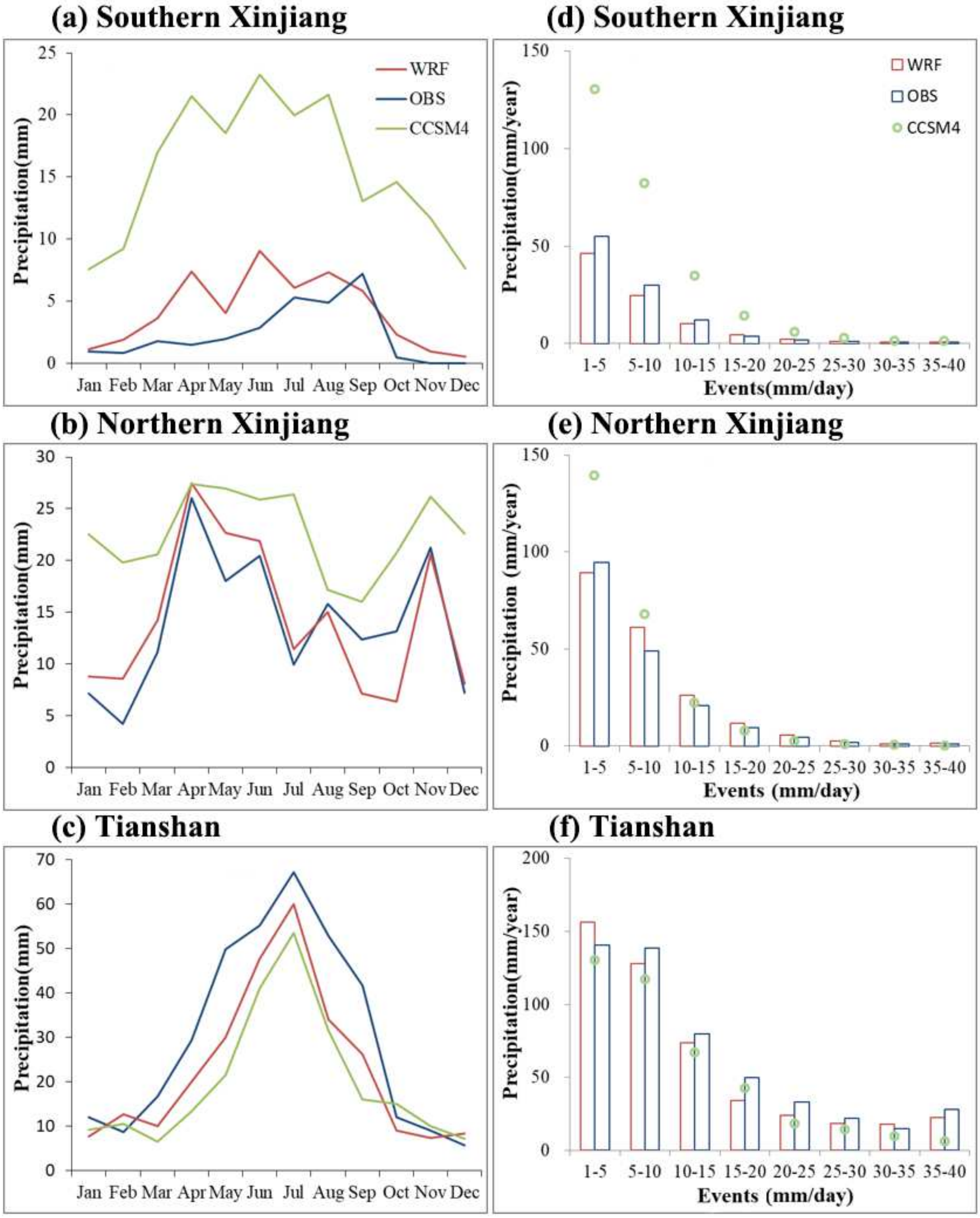

Fig. 3. Annual cycle of precipitation (units: mm/d) and precipitation intensity distribution in three subregions of Xinjiang during 1986–2005

3.2 Annual precipitation

Figs. 4a and f show the changes in annual precipitation simulated by thr WRF model under RCP4.5 and RCP8.5 for the mid-21st century (2040–2059), in terms of the difference from the present annual precipitation. These differences exhibit a general increases in annual precipitation inr most areas and slight decreases in some areas. These findings are consistent with the previously reported result that future the amount of precipitation will increase in China with the largest increase occurring in Northwest China (Gao et al., 2008). The variations in annual precipitation under RCP4.5 and RCP8.5 in Xinjiang suggest that wet conditions will continue. Under RCP4.5 (Fig. 4a), this increase has more orographic features than under RCP8.5, with the largest increases along the Tianshan and Altay Mountain. Meanwhile, in the Kunlun Mountains located in the northwestern Tibetan Plateau, the precipitation amounts exhibit a decreasing trend. Under RCP8.5 (Fig. 4f), although the precipitation still shows an increasing trend, the precipitation magnitudes significantly differ from those under the RCP4.5 scenario (Table 2). The areas with the largest increases in precipitation are still the Tianshan and Altay Mountains, whereas largest difference in precipitation occurs in the Kunlun Mountains, where the change in precipitation is exactly the opposite that under RCP4.5.

In addition, the second and third rows of Table 2 show the area-averaged changes in annual precipitation for the three subregions under RCP4.5 and RCP8.5, respectively. Relative to the present (1986–2005) precipitation, area-averaged increases in annual precipitation in Xinjiang in the 21st century are evident. These changes in annual precipitation show annual precipitation increased in all the three subregions. Compared with the precipitation amounts under RCP4.5, those under RCP8.5 show flat or smaller magnitudes of change over the Tianshan Mountains and Northern Xinjiang, and the only subregion with a continuous rise in annual precipitation through the decades is in the desert, Southern Xinjiang (Table 2). These changes are also observed in the spatial patterns of precipitation in Figs. 4a and f.

In the context of annual precipitation changes in Central Asia in the last 60 years, these results indicate that the current humid conditions in eastern Central Asia started in the mid-1980s, with the most significant being in Tianshan and Northern and Southern Xinjiang (Hu et al., 2002), will continue until this century.

Table 2: Differences in mean annual and seasonal precipitation between future (2040–2059) and present (1986–2005) conditions under RCP4.5 and RCP8.5 in three subregions (units: mm). The values in parentheses are percent differences from the precipitation amounts in 1986–2005.

	Scenario	Northern Xinjiang	Tianshan	Southern Xinjiang
ANN	**RCP4.5**	29.8 (13)	82.8 (15)	11.4 (11)
	RCP8.5	23.9 (12)	53.7 (11)	22.9 (22)
MAM	**RCP4.5**	16.2 (29)	30.6 (17)	6.5 (16)
	RCP8.5	8.4 (15)	16.2 (9)	6.7 (17)
JJA	**RCP4.5**	9.5 (20)	34.3 (21)	–1.5 (–3)
	RCP8.5	5.7 (9)	30.4 (21)	4.8 (13)
SON	**RCP4.5**	2.7 (5)	5.1 (6)	1.6 (10)
	RCP8.5	–0.7 (–1)	–0.4 (–1)	3.9 (22)
DJF	**RCP4.5**	1.4 (2)	12.8 (9)	4.8 (26)
	RCP8.5	10.5 (16)	6.5 (5)	7.5 (38)

3.3 Seasonal precipitation

The differences in projected seasonal precipitation in the mid-21st century from the present seasonal precipitation can be seen in Figs. 4b b–e and Figs. 4g–j for RCP4.5 and RCP8.5, respectively. Although the magnitude of increase in precipitation under RCP8.5 is smaller than that under RCP4.5, similar changes are observed both scenarios. The increases in precipitation under RCP4.5 and RCP8.5 in Tianshan mainly occur in spring and summer, and the amount of precipitation in spring and summer as a percentage of the increase in annual precipitation is 78.3% and 88.4%, respectively. Autumn and winter have smaller precipitation increases in Northern Xinjiang under RCP4.5 (Figs. 4d and e), whereas smaller precipitation increases mainly occur in summer and autumn under RCP8.5 (Figs. 4h and i). In Southern Xinjiang, the precipitation amounts tend to decrease relative to the present values under RCP4.5 in summer, and the area with the most significant decrease is located in the Kunlun Mountains (Fig. 4c). This feature is the main reason for the annual precipitation decrease in all of the Kunlun Mountains. Table 2 summarizes the area-averaged changes in seasonal precipitation relative to the present conditions in all three subregions.

Most of the area-averaged changes in seasonal precipitation are positive under RCP4.5 and RCP8.5, except that Northern Xinjiang and Tianshan have negative rates in autumn under RCP8.5 and Southern Xinjiang has a negative rate in summer under RCP4.5.

The changes in seasonal precipitation are mostly statistically significant at the 95% confidence level (based on the two-tailed Student's t-test), especially in mountainous areas such as the Tianshan, Altay, and Kunlun Mountains. The significance tests of precipitation relative to the present changes indicate that the areas that will experience the largest precipitation changes in the future in Xinjiang are likely the mountainous areas.

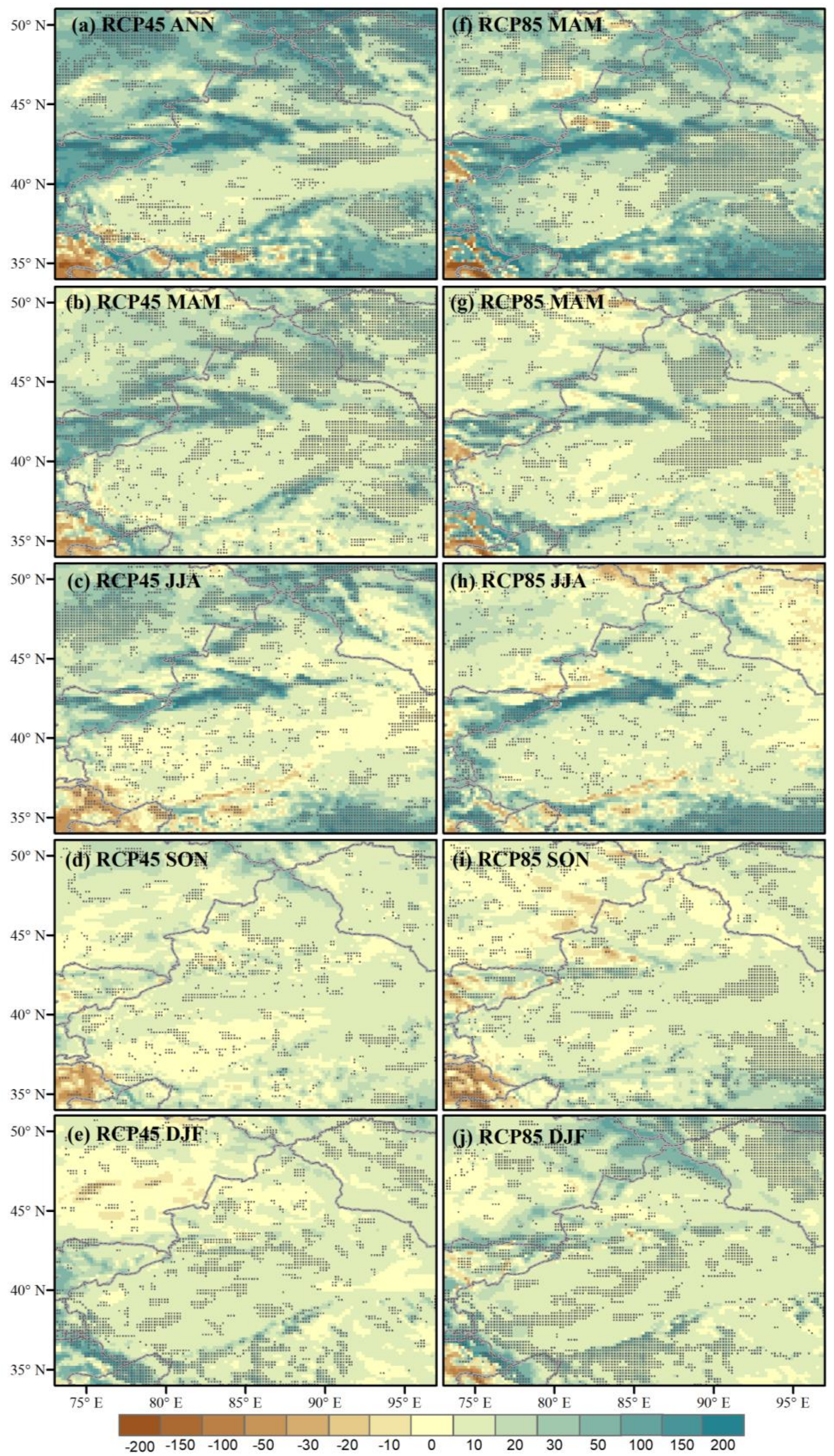

Fig. 4. Spatial distributions of the near-future difference (2040–2059 relative to 1986–2005) of annual, spring, summer, autumn, and winter precipitation under RCP4.5 (**a, b, c, d,** and **e,** respectively) and RCP8.5 (**f, g, h, i,** and **j, respectively**). The hatched areas indicate that the differences are significant at the 95% confidence level in a two-tailed Student's t-test (units: mm).

3.4 Daily precipitation

Daily precipitation events of different intensities compose the daily precipitation, which is a key aspect of the regional precipitation climate (Higgins et al., 2007). Fig. 5 shows the changes in daily precipitation events in terms of their contribution to the annual precipitation under RCP4.5 and RCP8.5 in the three subregions. Although light rain events (those with intensities less than 10 $mm\cdot d^{-1}$) will remain the main component in the future precipitation increase, the percentage of future heavy precipitation events (those greater than 30 $mm\cdot d^{-1}$) under both RCP4.5 and RCP8.5 is significantly greater than that of the light rain events, especially in Northern Xinjiang and Southern Xinjiang. This result is consistent with the change trend of the precipitation patterns in Xinjiang (Yuan et al., 2017; Zhang et al., 2012). All precipitation changes passed the 95% confidence level test. Note that the Tianshan has a relatively flat curve because this region has a large precipitation base across the entire spectrum, and the precipitation increment in each intensity category accounts for a relatively small part of its base value. Under RCP4.5 and RCP8.5, the increase in strong events and decrease in the contribution of light events to the annual precipitation in Xinjiang are similar to the global average trends detected in the GCM results of this century (Fischer and Knutti, 2016; Hennessy et al., 1997).

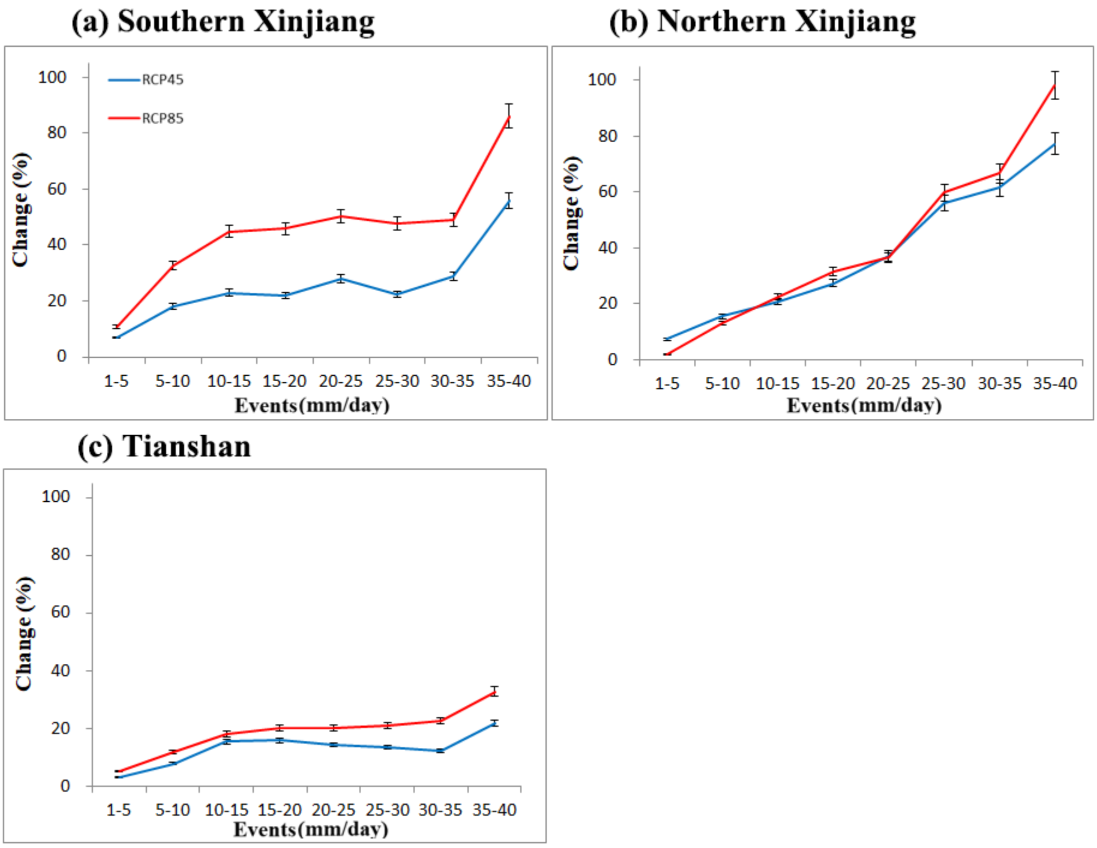

Fig. 5. Average percent change in intensity distribution of future (2040–2059) daily precipitation events in three subregions under RCP4.5 (blue line) and RCP8.5 (red line) from the average of 1986–2005.

3.5 Possible mechanism

To elucidate the possible mechanism of the future precipitation changes in the WRF simulations, we studied several key thermodynamic and dynamic fields including 500 hpa (which was used instead of 850 hPa because of the elevated orography of Xinjiang) geopotential as well as the relative vorticity, vertically integrated column precipitation (PW), and relative humidity (RH) under the RCP4.5 and RCP8.5 scenarios.

Fig. 6 shows the future seasonal changes in PW and 500 hPa air temperature under RCP4.5 and RCP8.5 relative to the present. Based on the Clausius–Clapeyron relationship (O'Gorman and Muller, 2010; Pall et al., 2007), as the emission scenario increases from RCP4.5 to RCP8.5, the air temperature continues to rise in each season, leading to a continuous increase in PW. In contrast to the absence of continuous increases in annual and seasonal precipitation from RCP4.5 to RCP8.5 (Fig. 4 and Table 2), the continuous rise in PW in the same period suggests that the PW is not a strong factor affecting changes in precipitation. However, Fig. 5 reveals that the increase in strong events in Xinjiang under RCP4.5 is smaller than under RCP8.5. As previous studies have shown, these differences are related to the PW (Fig. 6), because PW has been indicated to affect a rise in the number of extreme rainfall events in warm climates (Fischer and Knutti, 2016; Lehmann et al., 2015; Lenderink and Van Meijgaard, 2008).

Fig. 7 shows the future seasonal changes in RH at 500 hPa relative to the present. In contrast to PW, the seasonal changes in RH have many characteristics consistent with the seasonal changes in precipitation (Fig. 4). For example, the decrease in RH in the northwest of Tianshan is consistent with the changes in precipitation, especially in spring, summer, and autumn under RCP8.5, and the reduction in summer precipitation in the Kunlun Mountains in southern Xinjiang under RCP4.5 is consistent with the decrease in RH. Moreover, the increases in future precipitation in Northern and Southern Xinjiang are consistent with the increases in RH (as can be observed by comparing Figs. 4 and 7). The difference between the relationships between precipitation and RH and between precipitation and PW may originate from the fact that the PW is a strong function of the atmospheric temperature, via the Clausius–Clapeyron relationship. The warm temperatures of the next few decades will determine increase the moisture content in the atmosphere (Panthou et al., 2014), which will lead to an increase in PW. However, the atmospheric RH is relatively stable (i.e., given a sufficient time after the air temperature rises), the RH will return to its previous value (Ivancic and Shaw, 2016; Manabe and Wetherald, 1967). This characteristic of the atmospheric RH and its strong relationship with precipitation are consistent with our results, which indicate that the scale of future precipitation changes is limited (Figs. 4 and 5), although a considerable increase in atmospheric PW results in more intense precipitation during rainfall (Fig. 5).

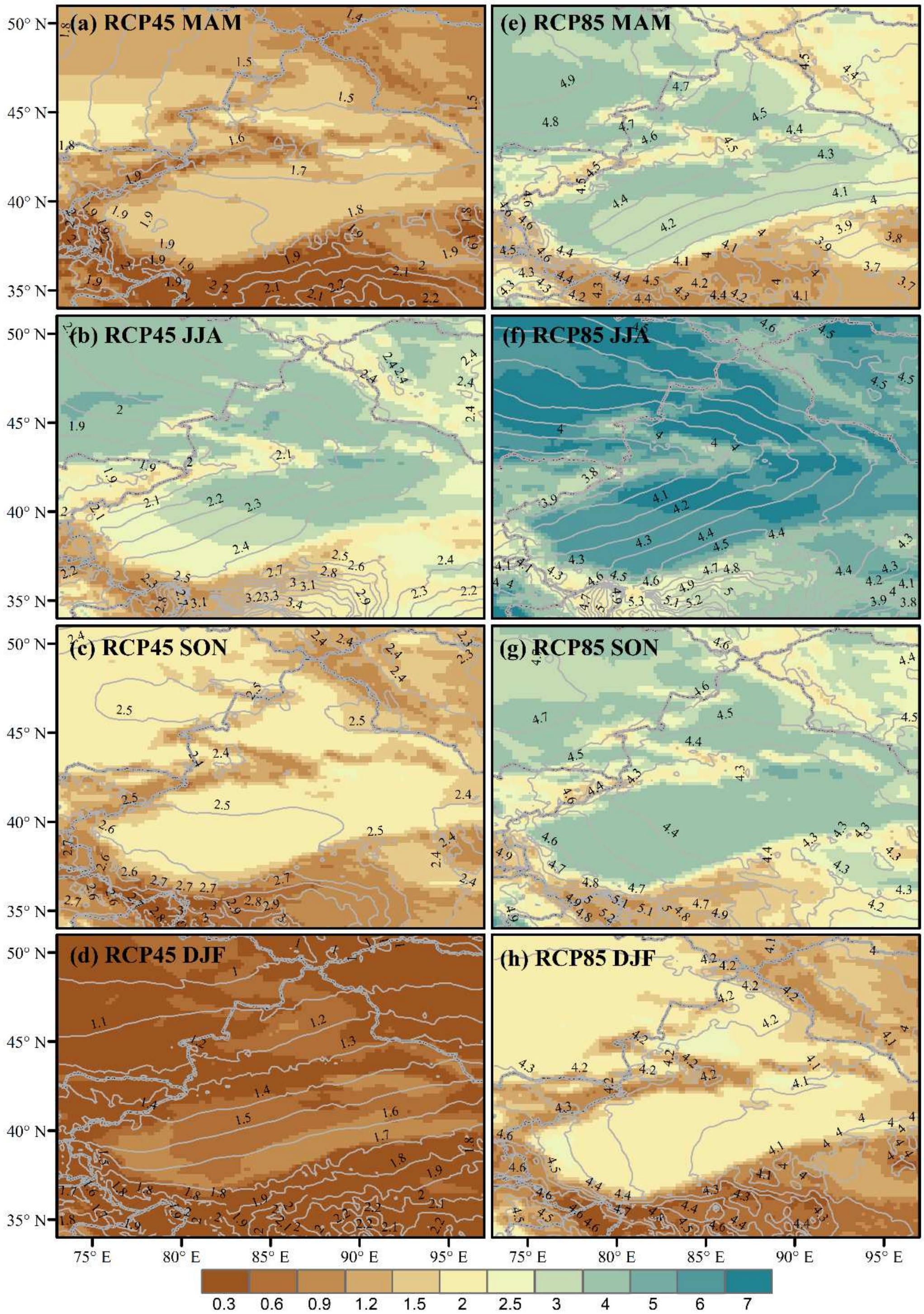

Fig. 6. Differences in PW (color scale, units: kg·m^{-2}) and 500-hPa air temperature (contour line, line interval 0.1 K) averaged under RCP4.5 and RCP8.5 in the future relative to the present day.

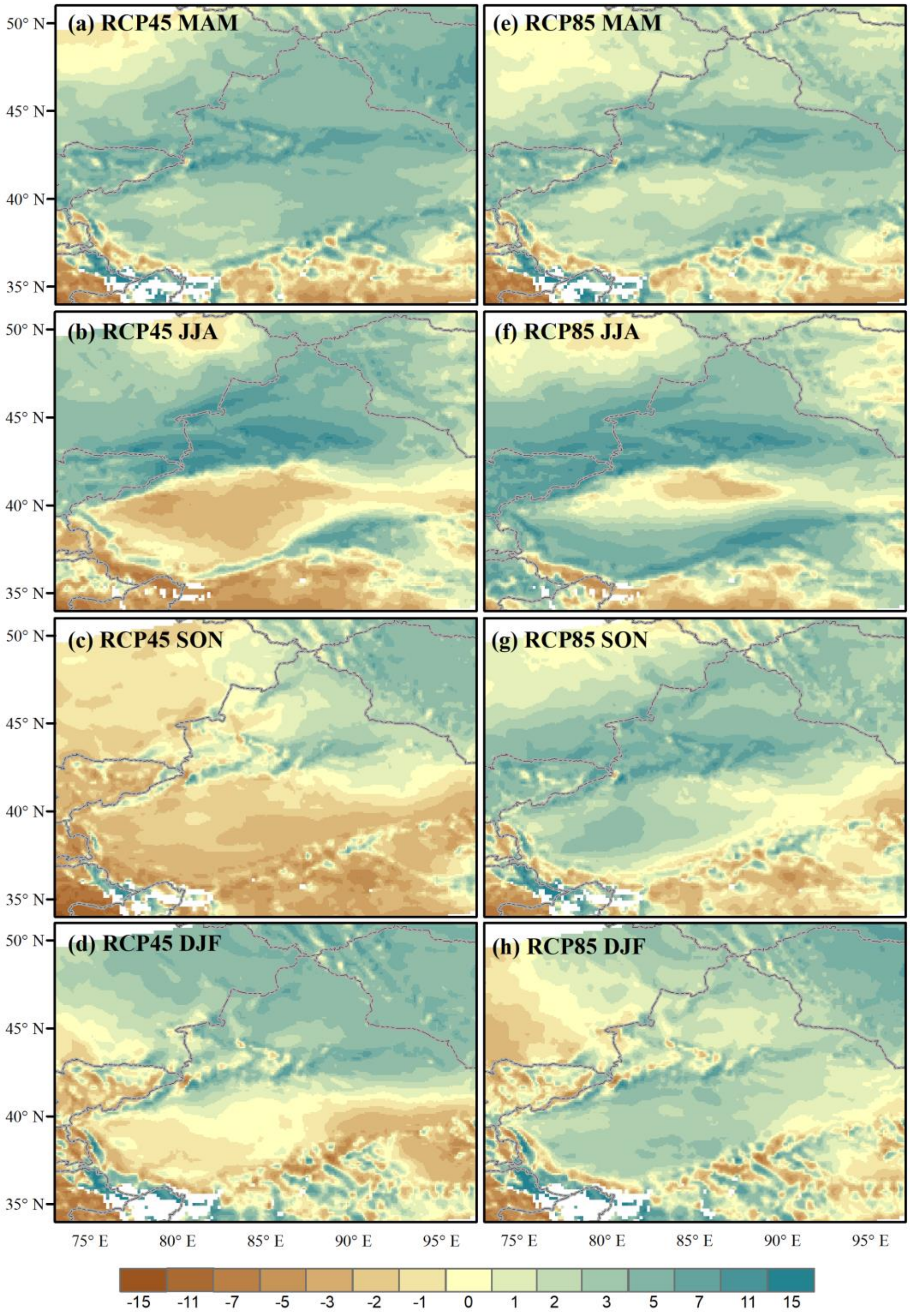

Fig. 7. Differences in 700 hPa RH (units: %) averaged under RCP4.5 and RCP8.5 in the future relative to the present day.

Future spatial variations in precipitation and RH largely depend on the potential for vertical motion in the circulation. From the perspective of vorticity, positive relative vorticity is conducive to vertical upward movement and precipitation (Dodla and Ratna, 2010). Fig. 8 shows the changes in relative vorticity (ζ) and geopotential height (ϕ) in the lower troposphere. ϕ has an upward trend in the future decades, and its spatial variations reveal the dynamic processes and ζ ($\sim\nabla^2\phi$). Focusing on the summer, Fig. 8b shows slightly more positive vorticity associated with low geopotential in most of Xinjiang, where less precipitation is expected in summer under RCP4.5 (Fig. 6b). In contrast, under RCP8.5, Fig. 8f shows more positive vorticity and low geopotential over Xinjiang, corresponding to strong increases in precipitation magnitude across the region (Fig. 6f). Compared with the present, the change in relative vorticity under RCP4.5 is significantly larger than that under RCP8.5. This difference will likely cause the amount of precipitation to be lower under RCP8.5 than under RCP4.5. Moreover, the geopotential of Xinjiang will continue to increase under RCP4.5 and RCP8.5. Compared to RCP4.5, the increase in geopotential will be more obvious under RCP8.5, which may suppress the occurrence of precipitation. In summer, the changes in geopotential height are smaller than those in winter and the changes in water vapor are generally larger (Figs. 6 and 8), which explains why there are more areas in which precipitation increases in summer and the opposite situation occurs in winter. The suppression of precipitation by the positive geopotential is obvious particularly over the Kunlun Mountains in summer, where the precipitation decreases. The positive anomalous geopotential heights are strengthened in each season under RCP8.5, which explains why the precipitation decreases are much larger under the RCP8.5 than under RCP4.5, although there is abundant water vapor in the atmosphere. Similar relationships between precipitation and ϕ and ζ are found in the transition seasons as well.

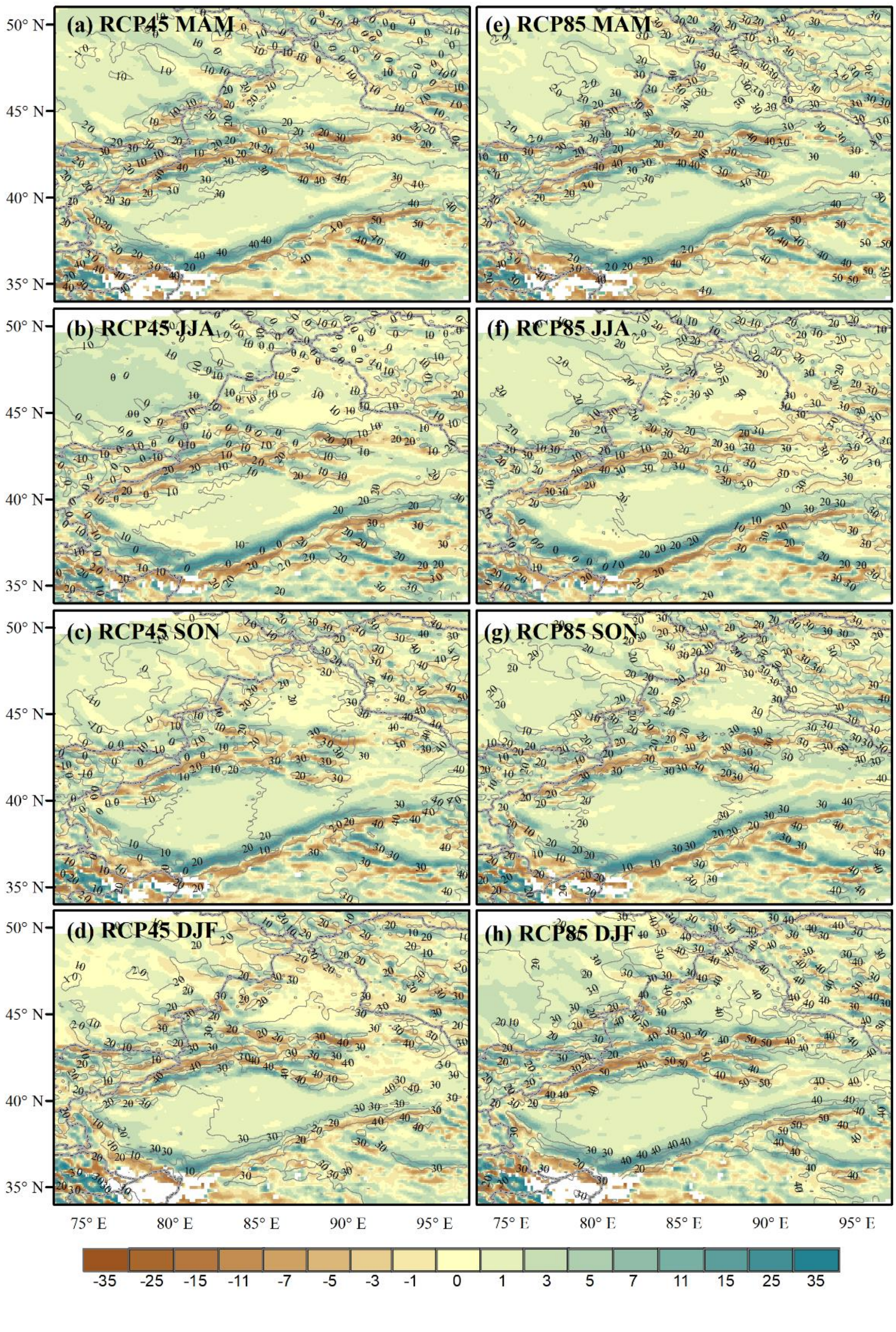

Fig. 8. Differences in relative vorticity (color scale, unit: 10^{-5} s^{-1}) and 500-hPa geopotential (contour line, line interval 10 $m^2 \cdot s^{-2}$) averaged under RCP4.5 and RCP8.5 relative to the present day. The white area is underneath the ground.

These variations in large-scale dynamic processes provide a mechanism for configuring instabilities and vertical motion for the projected changes in seasonal and annual precipitation in Xinjiang, in addition to a moisture advection effect suggested by Huang et al., (2014) based on their analysis of GCM outputs.

4. Discussion

Previous studies have suggested that, when compred with common datasets such as the Global Precipitation Climatology Centre (Schneider et al., 2018), the Climatic Research Unit Timeseries (Harris et al., 2014) and Asian Precipitation-Highly-Resolved Observational Data Integration Towards Evaluation（APHRODITE) (Yatagai et al., 2012), the MERRA dataset is more suitable for reanalyzing the precipitation in Central Asia (Hu et al., 2016). The reason is that the MERRA dataset has the advantages of better performance and minimal uncertainty, benefitting from the integration of satellite observations during the development of the dataset (Rienecker et al., 2011; Xu et al., 2020). In addition, although some remo-tely sensed dataets, such as theTropical Rainfall Measurement Mission (Kummerow et al., 1998)、Global Precipitation Measurement (Hou et al., 2014), the Climate Prediction Center Morphing Technology dataset (Joyce et al., 2004), have higher accuracy than the reanalysis dataset, remotely sensed datasets suffer from difficulty and inaccuracy when applied to describe the precipitation in the winter months (Ferraro et al., 1998; Zhang et al., 2018). Based on these considerations, we choose the MERRA dataset to verify the effectiveness of the downscaling of the WRF model in this study.

In this study, there was a relatively large difference in the simulated results achieved by the WRF and CCSM4 models when applied to Northern and Southern Xinjiang (Fig. 3). These differences are due to the different internal physical parameterization schemes used in the WRF and CCSM4 models. This type of discrepancy was also found during the dynamic downscaling process, which indicates that physical parameterization scheme employed for dynamical downscaling has can affect the biases intrinsic to the models (Zou et al., 2016).With the advance in spatial resolution of 10 km, more details about the small-scale local climate can be obtianed using the WRF rather than the CCSM4 model. For instance, the WRF model improved the simulated spatial precipitation patten. Owing to this improment, the boundaries of the high rainfall areas in the Tianshan Mountains and Altai Mountains were well simulated in our experiments (Figs. 2 and 4) (Chen et al., 2019; Qiu et al., 2017). Therefore, although the WRF model overestimated the precipitation in Northern and

Southern Xinjiang and underestimated the precipitation in Tianshan, it could estimate the precipitation tendency more accurately than the CCSM4 data (Fig. 3) (Chen et al., 2019; Qiu et al., 2017).

The unique spatial shpae of the mountain basin in Xinjiang has greatly affected the water vapor transport and distribution in Xinjiang (Yu et al., 2003). Specifically, the Tianshan Mountains block the moisture present in the northwesterly or northerly winds blowing from the Aral, Caspian, Black, and Mediterranean seas as well as the Arctic Ocean. Similarly, the Himalayas and Tibetan Plateau block most of the moisture coming from the south(Baldwin and Vecchi, 2016; Chen et al., 2019). Therefore, the geographical distribution of precipitable water vapor in Xinjiang (Fig. 4) differs from the spatial distribution of actual precipitation (Fig. 6), indicating that the precipitation in Xinjiang may be closely related to the water vapor transported by atmospheric circulation (Shi and Sun, 2008). It may be that, with increasing elevation, the amounts of precipitation in the Tianshan and Altay Mountains increase, whereas that along the north border of Tibetan Plateau decreases (Aizen et al., 2006; Baldwin and Vecchi, 2016; Guan et al., 2019).

5. Conclusions

This study was primarily focused on investigates the changes in the intensity and frequency of precipitation in Xinjiang in the near future. A regional climate model called the WRF model was used to downscale the CCSM4 model in Xinjiang for the present (i.e., 1986–2005) and near future (i.e., 2040–2059) under the RCP4.5 and RCP8.5 scenarios. The following conclusions can be obtianed from the results.

The annual precipitation will continue to increase under the RCP4.5 and RCP8.5 scenarios, and Tianshan has the largest increment among the three experimental regions. The increasing precipitation in the experimental regions excluding Southern Xinjiang, are much smaller under RCP8.5 than under RCP4.5. The projected annual precipitation in Xinjiang under both RCP4.5 and RCP8.5 suggests that the present wet and warm conditions will likely continue into the future, especially in Tarim Basin. The largest increase in annual precipitation will be in the mountainous areas from the Tianshan to Altay Mountains, with values ranging from 50 to 150 mm more than the present levels.

The seasonal precipitation in Xinjiang has remarkable characteristics of increased summer rainfall and decreased winter precipitation under both RCP4.5 and RCP8.5 compared to the present levels. Moreover, the difference in the amount of precipitation between summer and winter is much larger under RCP4.5 than under RCP8.5. In addition, the largest increase in the amount of seasonal precipitation in the future will likely occur in spring and summer in Tianshan and Northern Xinjiang, whereas this phenomenon will occur in spring and winter in Southern Xinjiang.

The more frequent heavy precipitation events (30–40 $mm \cdot d^{-1}$) are expected to occur in various subregions of Xinjiang. This change in the intensity of precipitation may result in more events with heavy precipitation in a warming climate. The events with small amounts of precipitation will account for a large proportion of seasonal and annual precipitation events, reducing the impact of the increase in the number of strong precipitation events on the amounts of seasonal and annual precipitation.

Acknowledgments

This work was supported by the National Key Research and Development Plan (Grant No. 2017YFB0504205) and National Natural Science Foundation of China (41901318).

Figures

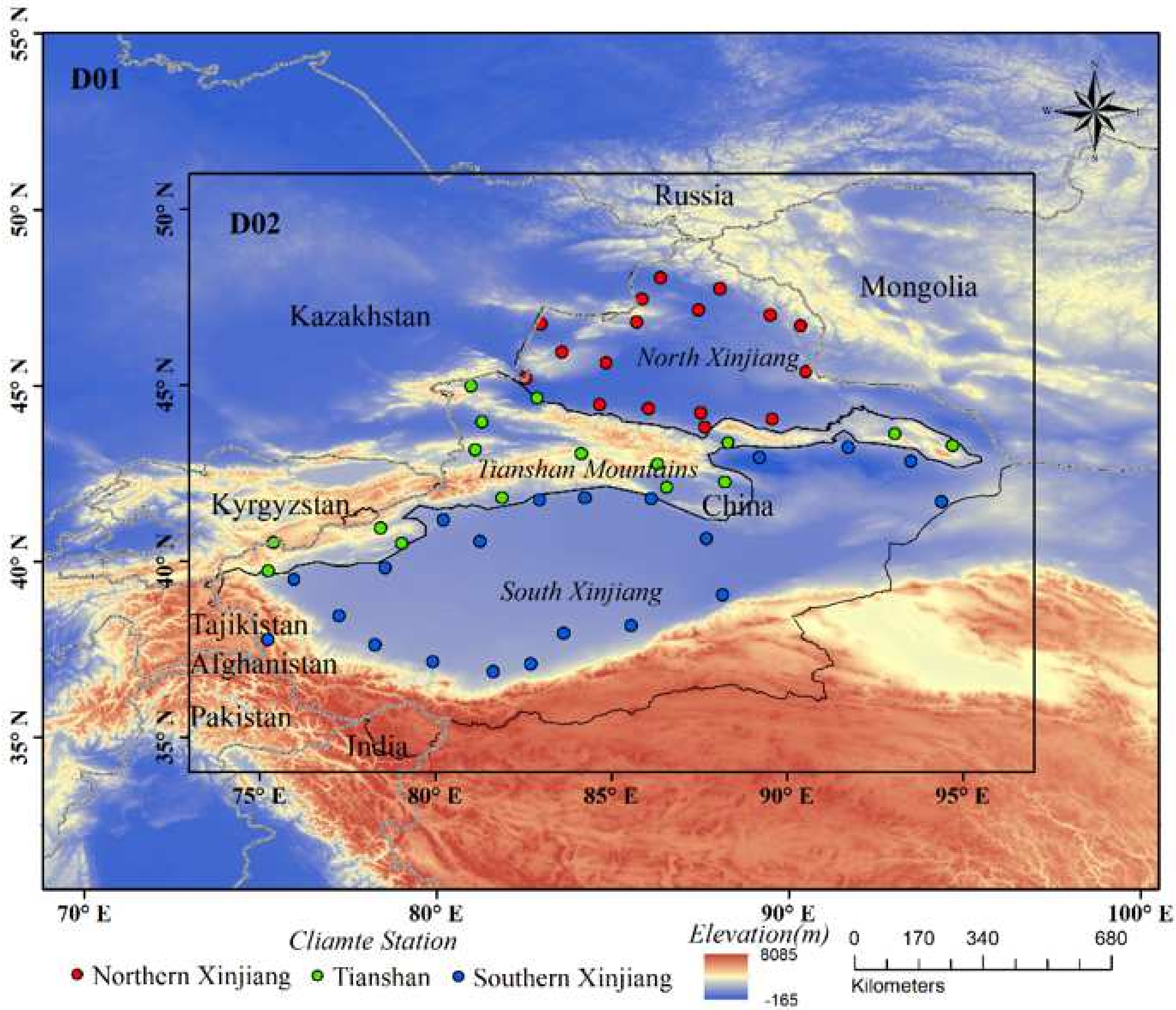

Figure 1

Simulated domain (D01) 50 km and (D02) 10 km of WRF and the ground meteorological stations with consistent precipitation variations in the study area (D02). Note: The designations employed and the presentation of the material on this map do not imply the expression of any opinion whatsoever on the part of Research Square concerning the legal status of any country, territory, city or area or of its authorities, or concerning the delimitation of its frontiers or boundaries. This map has been provided by the authors.

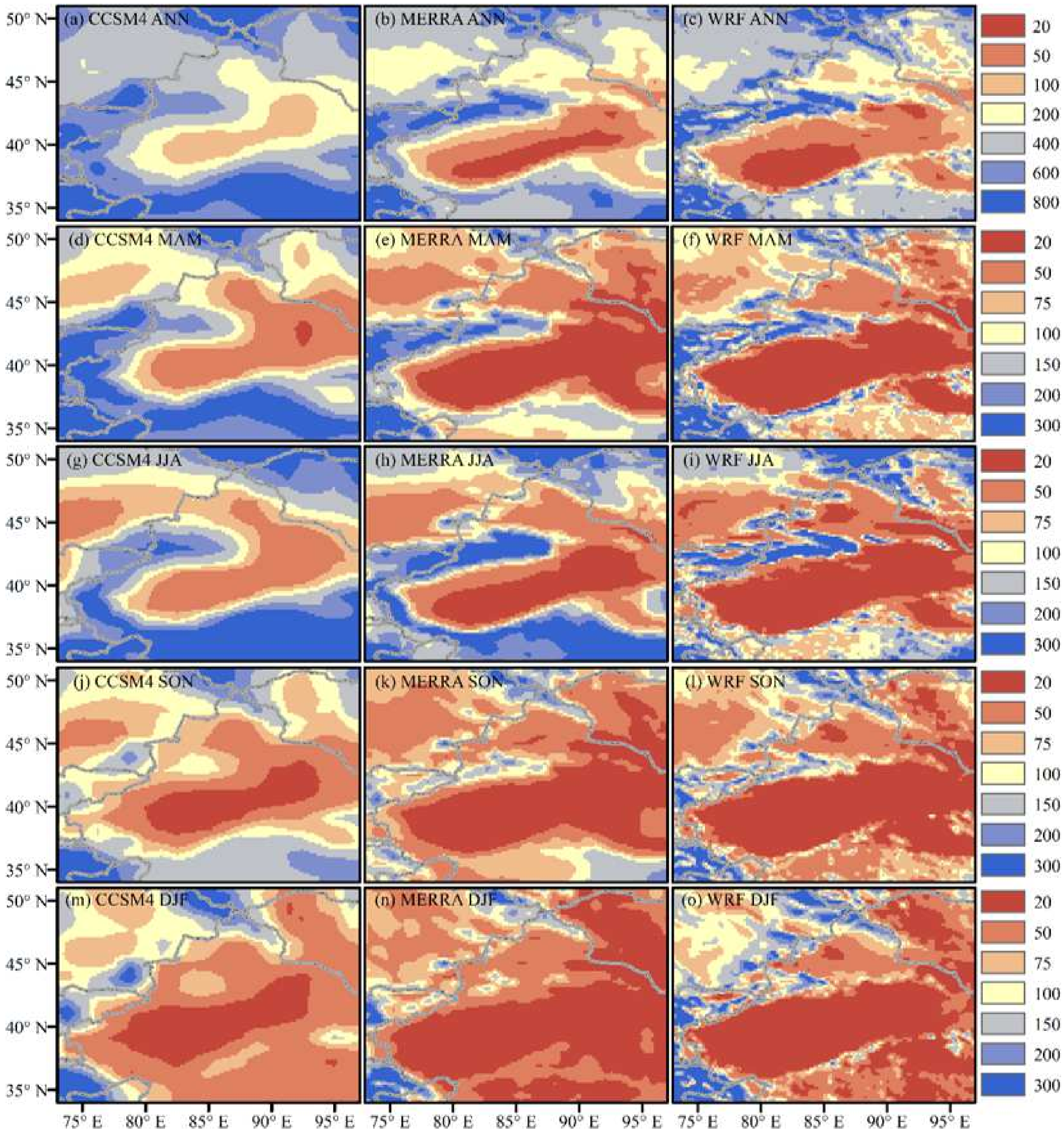

Figure 2

Mean annual and seasonal spatial patterns of precipitation for 1986–2005 derived from CCSM4 simulation (a,d,g,j,m), MERRA reanalysis data (b,e,h,k,n), and WRF simulation (c,f,i,l,o). ANN: annual (a–c), MAM: spring (d–f), JJA: summer (g–i), SON:autumn (j–l), DJF: winter (m–o). Note: The designations employed and the presentation of the material on this map do not imply the expression of any opinion whatsoever on the part of Research Square concerning the legal status of any country, territory, city or area or of its authorities, or concerning the delimitation of its frontiers or boundaries. This map has been provided by the authors.

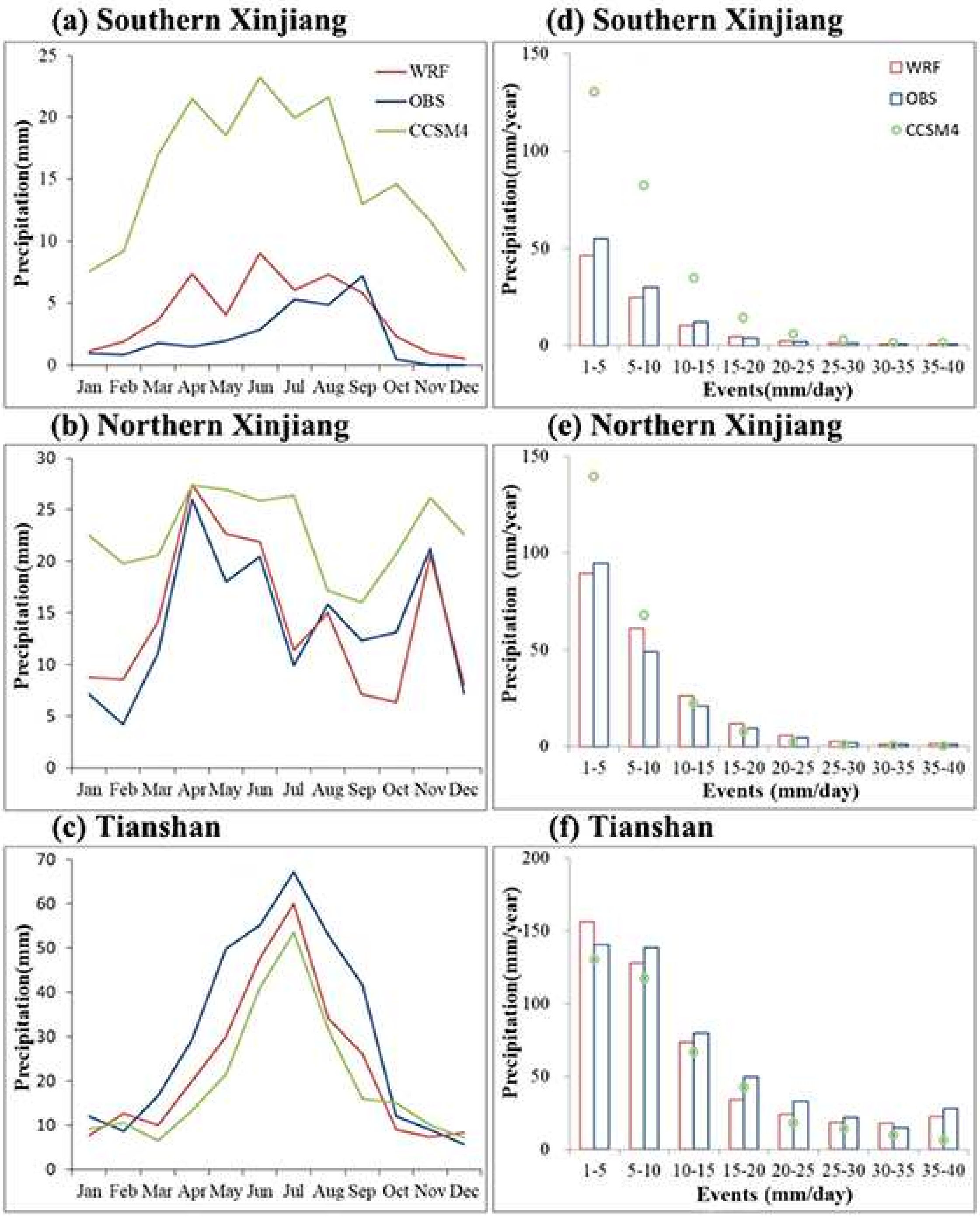

Figure 3

Annual cycle of precipitation (units: mm/d) and precipitation intensity distribution in three subregions of Xinjiang during 1986–2005

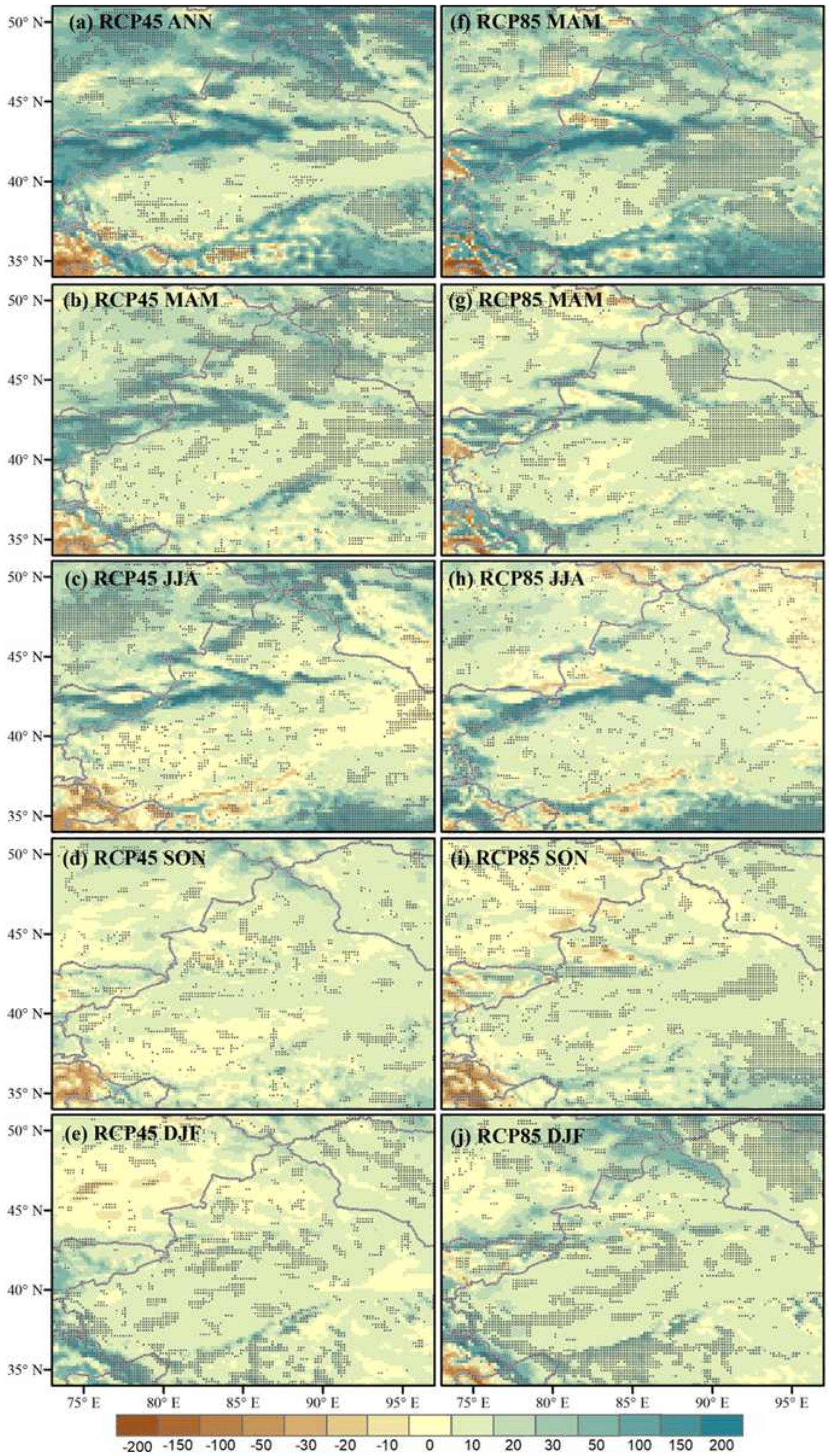

Figure 4

Spatial distributions of the near-future difference (2040–2059 relative to 1986–2005) of annual, spring, summer, autumn, and winter precipitation under RCP4.5 (a, b, c, d, and e, respectively) and RCP8.5 (f, g, h, i, and j, respectively). The hatched areas indicate that the differences are significant at the 95% confidence level in a two-tailed Student's t-test (units: mm). Note: The designations employed and the presentation of the material on this map do not imply the expression of any opinion whatsoever on the part of Research Square concerning the legal status of any country, territory, city or area or of its authorities, or concerning the delimitation of its frontiers or boundaries. This map has been provided by the authors.

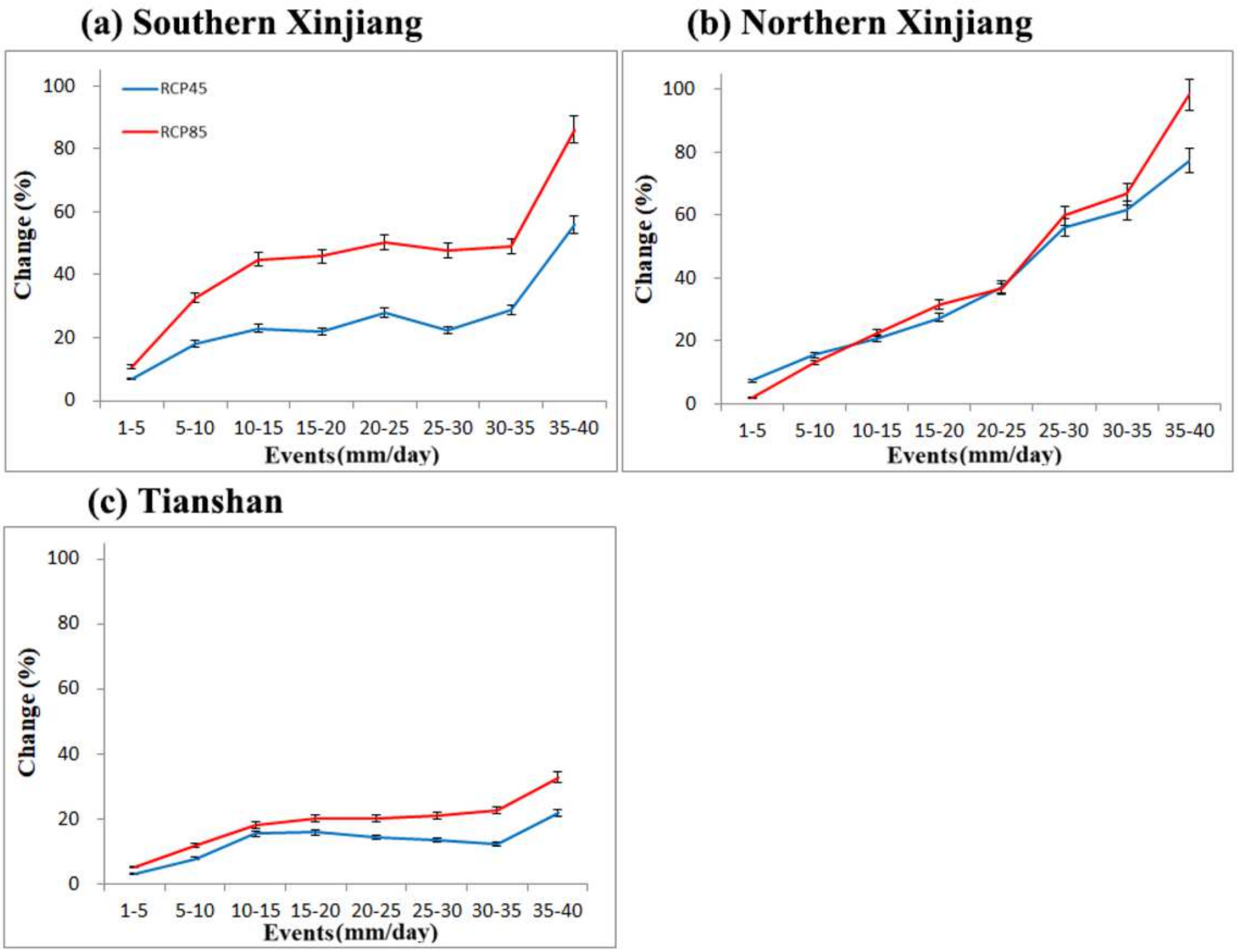

Figure 5

Average percent change in intensity distribution of future (2040–2059) daily precipitation events in three subregions under RCP4.5 (blue line) and RCP8.5 (red line) from the average of 1986–2005.

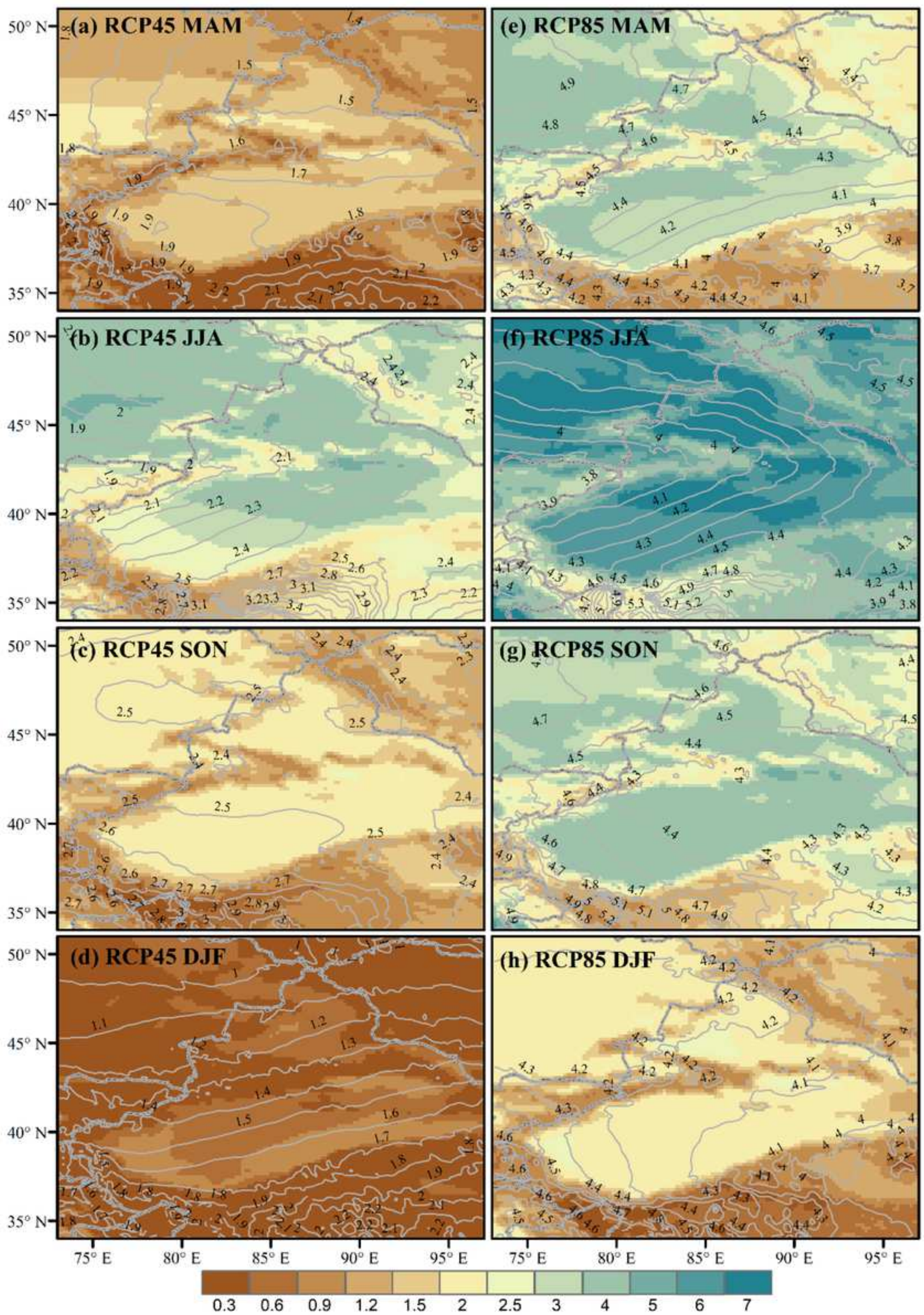

Figure 6

Differences in PW (color scale, units: kg·m-2) and 500-hPa air temperature (contour line, line interval 0.1 K) averaged under RCP4.5 and RCP8.5 in the future relative to the present day. Note: The designations employed and the presentation of the material on this map do not imply the expression of any opinion whatsoever on the part of Research Square concerning the legal status of any country, territory, city or area or of its authorities, or concerning the delimitation of its frontiers or boundaries. This map has been provided by the authors.

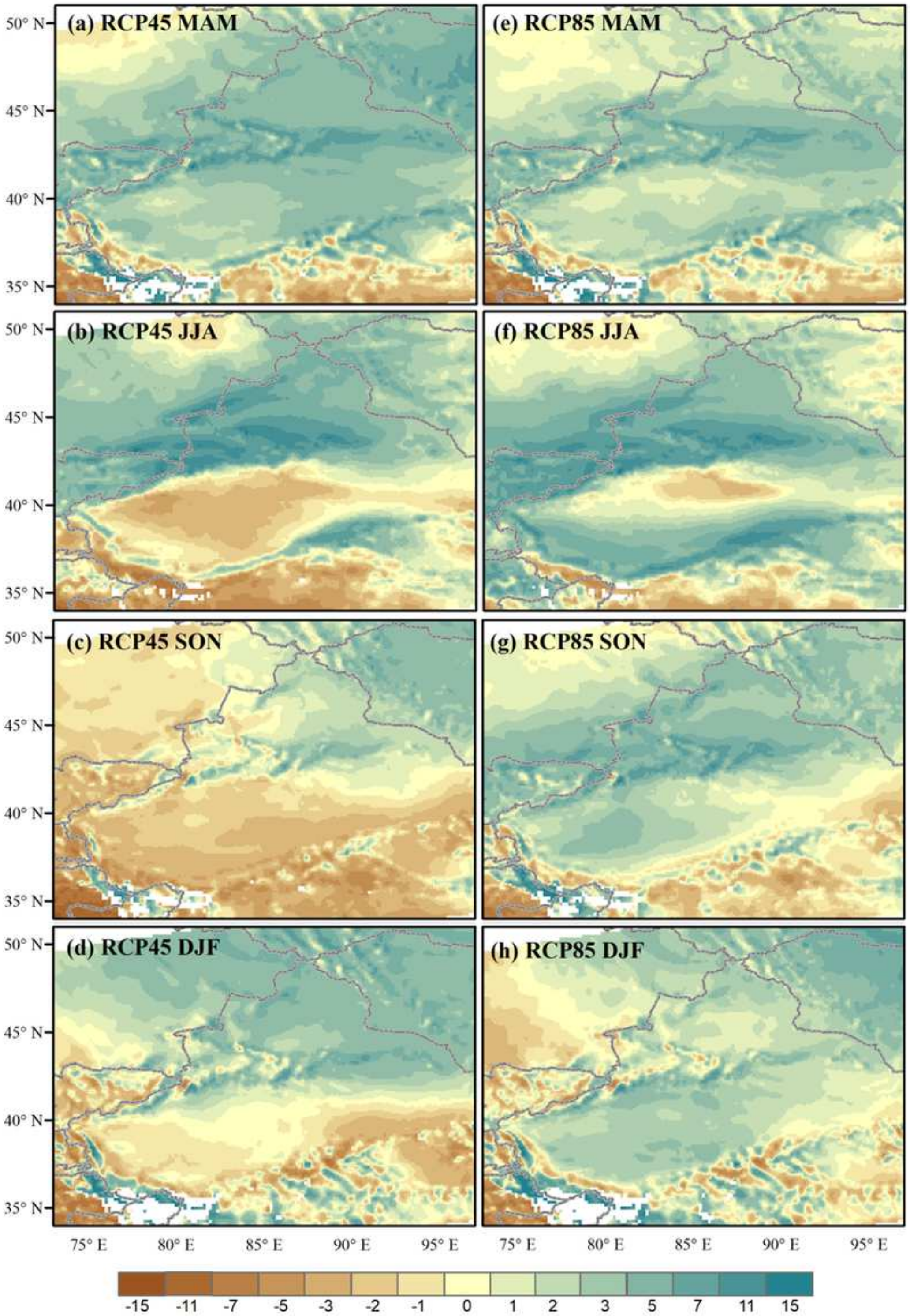

Figure 7

Differences in 700 hPa RH (units: %) averaged under RCP4.5 and RCP8.5 in the future relative to the present day. Note: The designations employed and the presentation of the material on this map do not imply the expression of any opinion whatsoever on the part of Research Square concerning the legal status of any country, territory, city or area or of its authorities, or concerning the delimitation of its frontiers or boundaries. This map has been provided by the authors.

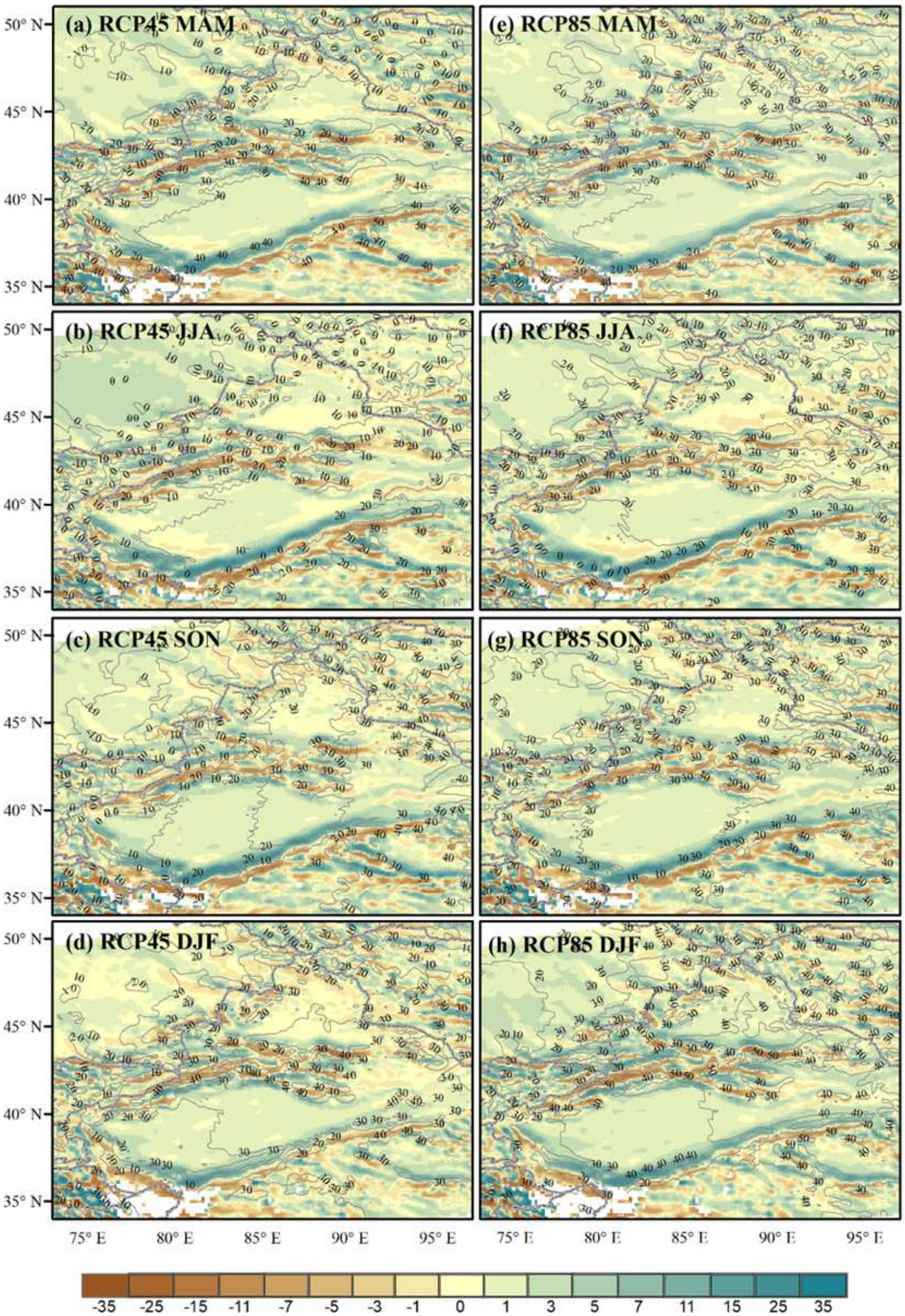

Figure 8

Differences in relative vorticity (color scale, unit: 10-5 s-1) and 500-hPa geopotential (contour line, line interval 10 m2·s-2) averaged under RCP4.5 and RCP8.5 relative to the present day. The white area is underneath the ground. Note: The designations employed and the presentation of the material on this map do not imply the expression of any opinion whatsoever on the part of Research Square concerning the legal status of any country, territory, city or area or of its authorities, or concerning the delimitation of its frontiers or boundaries. This map has been provided by the authors.